Available online at www.sciencedirect.com

SciVerse ScienceDirect

Ceramics International 38 (2012) 6327–6334

CERAMICS INTERNATIONAL

www.elsevier.com/locate/ceramint

Microstructure tailoring of the nickel–yttria stabilised zirconia (Ni–YSZ) cermet hollow fibres

Xiuxia Meng[a,b], Naitao Yang[a], Bo Meng[a], Xiaoyao Tan[a,c,*], Yimei Yin[b], Zi-Feng Ma[b], Jaka Sunarso[d]

[a]School of Chemical Engineering, Shandong University of Technology, Zibo 255049, China
[b]School of Chemistry and Chemical Engineering, Shanghai Jiao Tong University, Shanghai 200240, China
[c]Department of Chemical Engineering, Tianjin Polytechnic University, Tianjin 300160, China
[d]Australian Research Council (ARC) Centre of Excellence for Electromaterials Science, Institute for Frontier Materials, Deakin University, Burwood, VIC 3125, Australia

Received 27 March 2012; received in revised form 1 May 2012; accepted 1 May 2012
Available online 8 May 2012

Abstract

Nickel–yttria stabilised zirconia (Ni–YSZ) hollow fibres have been prepared by the phase inversion/sintering technique followed by a reduction process with hydrogen. This work is particularly focussed on tailoring the microstructure and the properties of hollow fibres by ethanol addition into the spinning hollow fibre suspension. Microstructure evolution change is demonstrated by increasing the amount of ethanol from 0 to 35 wt% e.g. the hollow fibre cross-section is modified from a sponge-like structure sandwiched by two thin finger-like layers to the sponge-like structure only. Higher ethanol content translates to denser hollow fibres. This trend also correlates with the shrinkage, mechanical strength and electrical conductivity of the hollow fibres. As the ethanol content is increased, shrinkage reduces, mechanical strength improves and electrical conductivity increases. The Ni–YSZ hollow fibres made from suspensions containing 15–25 wt% ethanol are considered the best option as anode supports for micro-tubular solid oxide fuel cells in terms of their median porosity values, since insufficient porosity would hinder the fuel and product transport, whereas excessive porosity would deteriorate the mechanical strength of the fibres.

Keywords: Hollow fibre; Solid oxide fuel cell; Anode; Phase inversion

1. Introduction

Fuel cells are attractive to convert chemical energy to electrical energy due to their high conversion efficiency. Since the conversion is performed without involving heat, the fuel efficiency for some fuel cells like solid oxide fuel cells (SOFCs) can reach up to 80% [1–4]. Among various fuel cells, polymer-electrolyte-membrane fuel cell (PEMFC) and SOFC have currently attracted most attention. PEMFCs are limited by their lower operating temperatures. SOFC, on the contrary, is an all solid-state device which conventionally operates between 600 and 1000 °C. Moreover, SOFCs also offer fuel flexibility (allows different fuel options such as hydrogen, natural gas, methane, gasoline and other hydrocarbons) as well as high tolerance to fuel impurities [1–4]. In recent years, hollow fibre or micro-tubular SOFCs (MT-SOFCs) featuring high volumetric power density, good mechanical properties, good thermo-cycling behaviour and quick start-up and shut-down operations have been developed [5–8]. Such MT-SOFCs are normally fabricated using a three-step process, i.e. preparation of anode micro-tubes, formation of a thin electrolyte film on the micro-tube outer surface and the deposition of cathode layers on the electrolyte film [6]. Yttria-stabilised zirconia (YSZ) is the most commonly used electrolyte material considering its high oxygen ionic conductivity, strong mechanical properties

*Corresponding author. Tel./fax: +86 533 2786292.
E-mail addresses: cestanxy@yahoo.com.cn (X. Tan), zfma@sjtu.edu.cn (Z.-F. Ma).

0272-8842/$36.00 © 2012 Elsevier Ltd and Techna Group S.r.l. All rights reserved.
http://dx.doi.org/10.1016/j.ceramint.2012.05.002

and good chemical compatibility. Accordingly, numerous MT-SOFCs have been prepared using Ni–YSZ as anode and YSZ as an electrolyte [9–12].

In MT-SOFC, anode micro-tube's architecture has a substantial role in fuel cell performance. While typical anode tubes are designed to have a thick wall layer to support the additional deposited layers with sufficient mechanical strength, this design, undoubtedly, leads to a large resistance to the diffusion of gaseous fuel and products during operation. To this end, an immersion induced phase inversion technique has been developed to fabricate ceramic hollow fibre membranes with a thin wall layer and an asymmetric structure [13–15]. The main advantages of this method lie primarily within the usage of inexpensive equipment and simple procedures which are of interest particularly towards reduced production costs of MT-SOFCs.

The phase-inversion method is a technique to prepare asymmetric membranes for gas separation applications [13–14]. The asymmetric membrane has a continuous sandwich microstructure consisting of a layer dominated by finger-like voids followed by a sponge-like layer and another layer dominated by finger-like voids [15–18]. Here, finger-like voids provide transport channels for gaseous fuel and products. The sponge-like structure, on the other hand, acts as three phase boundaries (TPB) required for electrochemical reactions while also providing necessary mechanical strength into the hollow fibres [19]. The optimum balance between finger-like voids and sponge-like structure is of interest since an excess amount of finger-like voids would interrupt the percolative path of electronically conductive Ni metal required to maintain stable anode performance. Therefore, microstructure tailoring of the anode hollow fibres is crucial to enhance the performance of MT-SOFCs.

In this work, phase inversion and sintering are used to prepare Ni/YSZ hollow fibres with different microstructures. The effect of the resultant microstructure on the mechanical strength, porosity and electronic conductivity of SOFC anodes is studied. These hollow fibre anodes are then utilised as base layers upon which further electrolyte and cathode layers are deposited to make micro-tubular fuel cells.

2. Experimental

2.1. Materials

Commercially available NiO and 8 mol% yttria-stabilized zirconia (8YSZ) powders with 99.9% purity and particle size diameters of 20–30 nm (Weifang Yitong Co. Ltd., Weifang, China) were used as the anode materials. Polyethersulfone (PESf) ((Radel A-300), Ameco Performance, USA), *N*-methyl-2-pyrrolidone (NMP) (AR Grade, $>99.8\%$, Kermel Chem Inc., Tianjin, China) were used as the polymer binder and the solvent to prepare the spinning solution.

2.2. Spinning of the NiO/YSZ hollow fibres

A starting solution was first prepared to spin the hollow fibre precursors. A calculated quantity of PESf was dissolved in the NMP/ethanol mixture solution in a 250 cm^3 bottle. The composition of NMP/ethanol solution was varied from 0 to 35 wt% (of NMP) with the increment of 5 wt%. After the polymer solution formed, a mixture of NiO and YSZ powders (which were dried at 120 °C for 12 h previously), were then added gradually under stirring. The stirring was carried out continuously for at least 48 h to ensure that all powders were dispersed uniformly in the polymer solution. The starting solution was de-gassed at room temperature for an hour and the solution was then transferred to a stainless steel reservoir and pressurised to 0.10 MPa (absolute pressure) using nitrogen. A spinneret with the orifice diameter/inner diameter of 3.0/1.5 mm was used to spin the hollow fibre precursors. De-ionised water and tap water were used as the internal and external coagulants, respectively. The formed hollow fibre precursors were immersed in a water bath for more than 24 h to complete the solidification process. The hollow fibre precursors were heated in a furnace at 800 °C for 200 min to remove the organic polymer binder followed by sintering at 1400 °C in ambient non-flowing air atmosphere for 5 h to allow the sufficient fusion and bonding. After cooling to room temperature, the resulting NiO/YSZ hollow fibres were kept in a dry place for subsequent characterisation and reduction. The operating conditions employed to prepare NiO/YSZ hollow fibres are summarised in Table 1.

2.3. Reduction of the Ni/YSZ anodes

To obtain Ni/YSZ anode tubes, the sintered NiO/YSZ hollow fibres were reduced using hydrogen. A quartz tube was used as the holder for the 4 cm-long NiO/YSZ hollow fibre samples. Argon was used as purge gas during ramping up to 200 °C; above which pure hydrogen was then passed through the chamber with a flow rate of 20 $cm^3\ min^{-1}$. The reduction was performed at 700 °C for 5 h. After cooling down to 200 °C, the samples were then purged again with argon until the temperature reached room temperature. The resultant porous Ni/YSZ anode tubes were characterised.

Table 1
Preparation conditions of the NiO/YSZ hollow fibres.

Experimental parameters	Values
Compositions of the starting solution (wt%)	
NiO/YSZ	58.3
PESf	8.3
NMP+ethanol	33.3
Spinning temperature (°C)	20
Nitrogen pressure (absolute pressure) (MPa)	0.1
Injection rate of internal coagulant ($cm^3\ min^{-1}$)	20
Air gap (cm)	1
Sintering time (h)	5

2.4. Characterisation methods

2.4.1. Scanning electron microscopy (SEM)

Morphologies of NiO/YSZ and Ni/YSZ hollow fibres were obtained using scanning electron microscopy (SEM) (FEI Sirion200, The Netherlands). Gold sputter coating was performed on the samples under vacuum prior to SEM imaging. The shrinkage of the anode micro-tubes at different sintering temperatures was calculated from SEM images.

2.4.2. Powder x-ray diffraction (PXRD)

The crystal phases of the prepared NiO/YSZ and Ni/YSZ hollow fibres were determined by x-ray diffraction (Bruker D8 Advance, Germany) using Cu-Kα radiation (λ=0.15404 nm). The hollow fibres were ground into powders prior to the XRD measurements. Continuous scan mode was used to collect data with 2θ between 20° and 80°, a 0.02° sampling pitch and a 2° min^{-1} scan rate. The X-ray tube voltage and current were set at 40 kV and 30 mA, respectively.

2.4.3. Porosity and pore size distribution

The porosity of hollow fibres was measured using a mercury porosimeter (Quantachome Instruments PM 60-6) employing a mercury pressure between 138 kPa and 275.8 MPa. Micrometrics software (version 1.09) was used to calculate the pore size distribution. Prior to measurements, the samples were heat-treated at 200 °C for 2 h. The weight of each sample for the measurements was around 1.0 g. The porosity of the hollow fibres was calculated from the bulk density obtained from the weight and the corresponding dimensions of the samples.

2.4.4. Mechanical strength

The mechanical strength of the hollow fibres was measured using a three-point bending instrument (Instron Model 5544) with a cross-head speed of 0.5 mm min^{-1}. Hollow fibre samples were fixed on the sample holder at a distance of 32 mm. The bending strength (σ_F) was calculated from

$$\sigma_F = \frac{8FLD}{\pi(D^4-d^4)} \quad (1)$$

where F is the force at which fracture takes place; L, D and d are the length (32 mm), the outer diameter and the inner diameter of the hollow fibres, respectively. The values of outer diameter (D) and inner diameter (d) were obtained from the SEM images.

2.4.5. Conductivity

The electrical conductivity of Ni/YSZ hollow fibres was measured at room temperature using a four-probe direct current (DC) method utilising an electrochemistry workstation (Zahner IM6ex). Silver wires attached at both ends of the sample by silver paste which acts as the current and voltage electrodes. Silver paste was applied to the sample and cured at 750 °C for an hour in hydrogen atmosphere. Current–voltage characteristics were recorded in the current range of 0–1.0 A. All samples showed linear I–V behaviour on which the electrical resistance was obtained from the slope of the I–V curves using the least square method. The electrical conductivity of the anode was estimated using

$$\sigma_{fibre} = \frac{L_{fibre}}{R_{fibre} \times A_{fibre}} \quad (2)$$

where R_{fibre} is the fibre resistance (Ω), L_{fibre} is the fibre length (cm) and A_{fibre} is the area for current flow (cm^2).

3. Result and discussion

By varying the ratio of solvent/polymer/ceramic oxide or by introducing additives such as polyvinylpyrrolidone (PVP) or by adding non-solvent such as ethanol, the viscosity of hollow fibre suspensions can be controlled which affects membrane morphology and properties [20–21]. Since ethanol is a good dispersant for ceramic powders, the dispersion of ceramic powders in the prepared hollow fibre is expected to be more uniform (relative to not using ethanol). The extent of ethanol addition to spinning suspensions; quantified as a percentage of the total NMP-ethanol content leads to viscosity change shown in Fig. 1. The suspension viscosity value of 20,900 cP for 0 wt% ethanol suspension slightly decreases to 20,650 cP when 5 wt% of ethanol is added which might be associated with insufficient ethanol amount to solvate the mixtures. However, increasing ethanol content to 10 wt% brings about increasing viscosity up to 27,400 cP which further increases to 29,300 and 32,500 cP for 15 and 20 wt% ethanol solutions, respectively. Further addition resulted in even larger viscosity increase e.g. 37,100, 46,250 and 49250 cP for 25, 30 and 35 wt% ethanol suspensions, respectively.

Fig. 2A-1 to E-1 feature the SEM images of cross-section of NiO–YSZ hollow fibre sintered at 1400 °C made using the 0, 10, 20, 30 and 35 wt% ethanol suspensions,

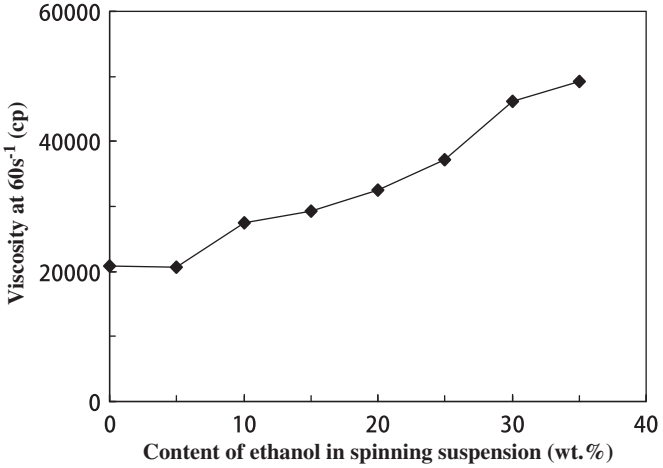

Fig. 1. Viscosity of spinning suspension as a function of ethanol content.

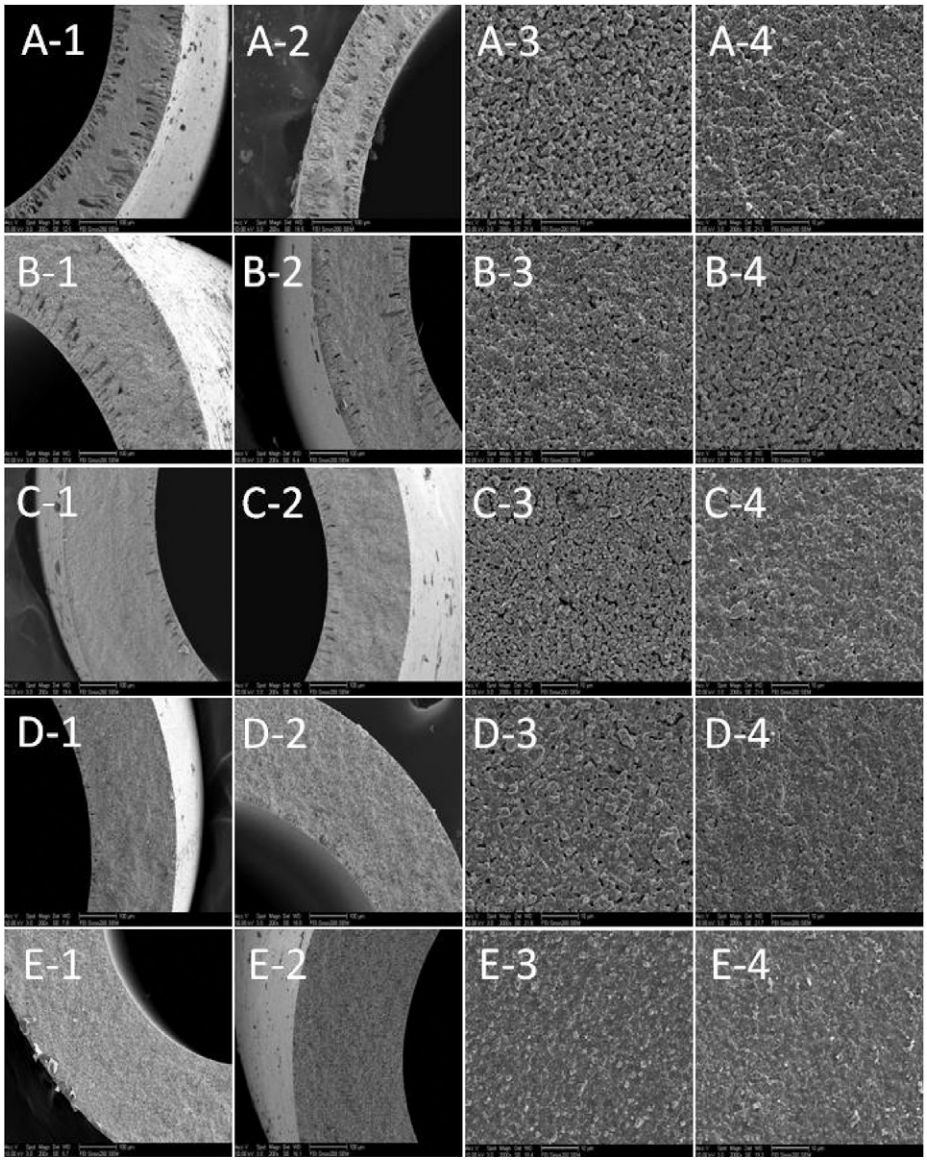

Fig. 2. Scanning electron microscopy (SEM) images of (1) cross-section of NiO/YSZ hollow fibres sintered at 1400 °C; (2) Ni/YSZ hollow fibres (after reduction); (3) inner surface and (4) outer surface. *A*, 0; *B*, 10%; *C*, 20%; *D*, 30%; *E*, 35%.

respectively. Hollow fibres made from 0 wt% ethanol solution have an asymmetric structure, with sponge-like structure dominating the central region of the hollow fibres as well as finger-like structures at the outer side occupying up to 40% of the fibre thickness and inner sides occupying up to 20% of the fibre thickness. The formation of such asymmetric structure is attributed to the rapid precipitation occurring at both inner and outer walls exposed to the coagulants, resulting in finger pores. The slow precipitation at the centre of the fibre layer, on the other hand, leads to the sponge-like structure [22]. Hollow fibre made from 10 wt% ethanol suspension has the same asymmetric structure as fibre A (0 wt% ethanol suspension) with reduced length of the finger-like structure sections on both inner and outer fibre surfaces. The addition of ethanol as a non-solvent brings about faster fibre precipitation during contact with the internal or outer coagulant since the polymer phase is brought closer to its precipitation point. The faster polymer precipitation tends to speed up the viscosity increase; thus inhibiting further viscous fingering and as a result, shorter finger-like voids are formed. The relative thickness of the finger-like layers in inner sides are further reduced to approximately 15%, 10%, 5% (of fibre A) and totally disappear when the ethanol content is increased to 10, 20 and 30 and 35 wt%, respectively (Fig. 2B-1, C-1, D-1 and E-1). The finger-like layer in the outer side of fibres, in contrast, is completely removed by utilising 20 wt% ethanol suspension. These observations demonstrate that the ethanol addition contributes two effects to the spinning suspension e.g. increases the initial suspension viscosity and decreases the precipitation rate. The second effect is primarily attributed to the larger solubility parameter for ethanol relative to NMP which causes slow precipitation [15]. Accordingly, these two

effects in combination bring about the formation of a larger sponge-like structure.

The cross section images of the Ni–YSZ hollow fibres (after reducing NiO–YSZ hollow fibres) are shown in Fig. 2A-2 to E-2. The cross-sectional structures of the initial hollow fibres (prior to reduction) are pretty much retained after reduction processes, suggesting that the reduction does not alter fibre macrostructure. Oxygen removal from NiO, nonetheless, provides a more porous structure, particularly in the sponge-like region. The external coagulant seems to be more effective than the internal coagulant (to induce coagulation) during solvent/non-solvent exchange in phase inversion process. This causes more rapid precipitation through the outer surface (relative to inner surface) as evidenced by the denser outer surface becomes relative to the inner surface (Compare Fig. 2A-3 with A-4, B-3 with B-4 up to E-3 and E-4).

Significant shrinkage of hollow fibres (e.g. shortened fibre length and wall thickness) occurred during the sintering process as a result of the organic binder removal and solid-state reaction between NiO and YSZ particles, in agreement with the previous report [23]. The shrinkage extent is normally a function of properties and particle size distribution of the ceramic–metallic powders, the weight ratio of ceramic–metallic powder to polymer binder and the sintering condition. The amount of finger-void in the structure, nonetheless, is also expected to affect the shrinkage as denoted by the observed shrinkage trend as a function of ethanol content in the suspension displayed in Fig. 3. This figure indicates that the shrinkage decreases from 44% to 20% by increasing the ethanol amount from 0 to 35 wt% with marginal reduction observed by adding ethanol beyond 25 wt%. The shrinkage is indeed influenced by the layer structure e.g. finger-like void and sponge layer. Despite negligible variation in hollow fibres dimensions after reduction, porosity and mechanical strength seem to be modified after reduction (will be discussed below).

As anode support for other SOFC components, hollow fibres should ideally provide sufficient pore channels for fuel and products transport required to sustain electrochemical reactions. Fig. 4 presents the porosity of NiO/YSZ and Ni/YSZ hollow fibres as a function of ethanol content in spinning suspensions measured using mercury porosimetry. The porosity decreases with increasing ethanol content (in spinning suspension); consistent with the previous SEM images. The porosity calculated from the bulk density of the hollow fibres is also plotted in Fig. 4 for comparison. The porosity values for hollow fibres made from suspensions containing less than 15 wt% ethanol closely resemble the calculated values. For hollow fibres made from suspensions containing more than 15 wt% ethanol, on the other hand, the calculated values lie above the measured values. Such discrepancy might be due to the formation of closed pores during the high temperature sintering process for hollow fibres made from high ethanol containing suspensions. Ideally, the optimum anode porosity is between 30% and

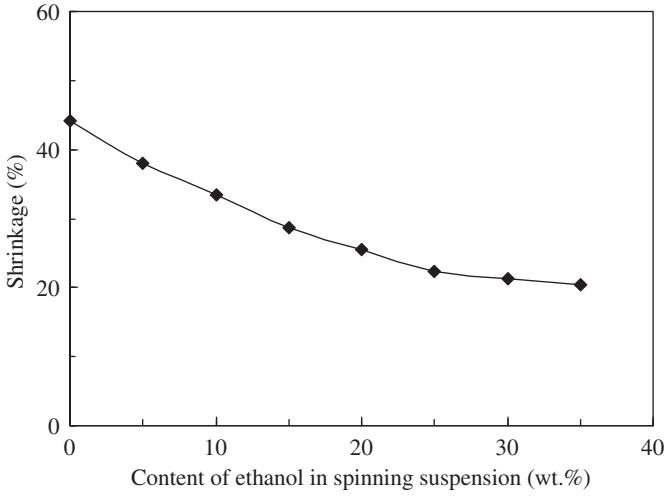

Fig. 3. Shrinkage (%) of the NiO-YSZ hollow fibres (using outer diameter).

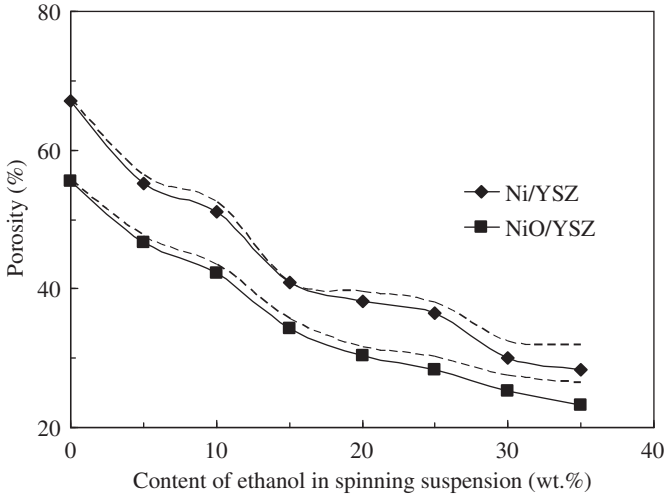

Fig. 4. Porosity of Ni/YSZ hollow fibres as a function of ethanol content.

40% (according to seepage flow theory) [24]. Therefore, the ideal ethanol amount would be between 15 and 25 wt% which in turn, provides porosity values between 40.85% and 36.5%.

Moreover, anode hollow fibres should provide sufficient mechanical strength. The mechanical strength of the hollow fibres is depicted in Fig. 5, on which the three-point bending value is plotted against ethanol content (in spinning suspension). The maximum strength of 400 MPa is shown by the densest NiO/YSZ fibre e.g. fibre made from 35 wt% ethanol suspension (which contains only sponge-like structure). With decreasing ethanol content (in suspensions) and sponge-like layer amount, the bending strength is reduced. Fibres made without ethanol in suspension have the lowest strength. Sponge-layer structure, to some extent, seems to contribute positively to the mechanical strength of the fibre. The reduction process substantially reduces the strength value. For example, the

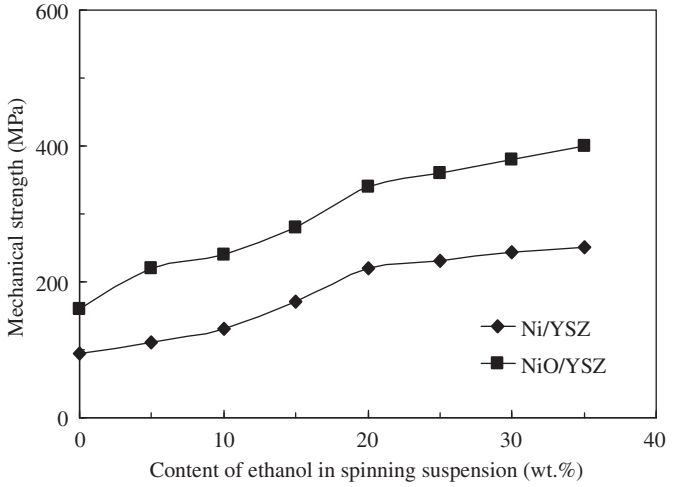

Fig. 5. Mechanical strength of NiO/YSZ and Ni/YSZ hollow fibres at different ethanol content.

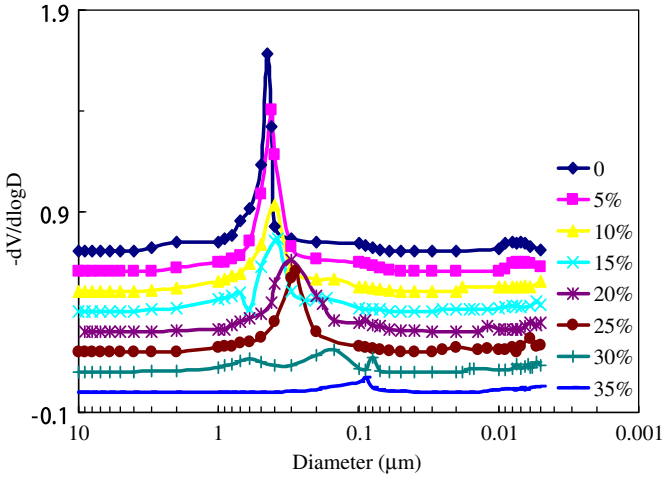

Fig. 6. Pore size distributions of Ni/YSZ hollow fibres as a function of ethanol content.

bending strength of the sintered Ni/YSZ hollow fibres made from 20 wt% ethanol suspension is 220 MPa, reduced by 110 MPa (relative to NiO/YSZ hollow fibres). The oxygen loss during reduction seems to contribute to the weakening of the bonds between ceramic–metallic particles as well as the enlarged bulk porosity; both of which causes substantial loss in mechanical strength. The lower mechanical strength value for the reduced Ni/YSZ hollow fibres, nonetheless, is still considered more than sufficient for SOFCs. Previous studies on the anode hollow fibres of similar size and Ni content, for example, report bending strength value of up to only 178 MPa [16,23]. Hollow fibres with bending strength above 150 MPa are normally considered sufficient in the point of view of mechanical strength, implying that hollow fibres prepared here using suspensions containing more than 15 wt% of ethanol can be used as supports for MT-SOFC.

Further insights on the hollow fibre microstructure can be attained by comparing the mercury intrusion data for each hollow fibre, shown in Fig. 6. Thus far, two types of pores have been observed initially e.g. finger-like voids and sponge-layer pores as well as additional pores formed later during NiO reduction. Fibres made from suspensions without ethanol exhibit pore size distribution containing peak centred at ~0.45 μm, most probably attributable to the finger-like voids. A peak at lower size of ~0.008 μm, on the other hand, most likely represents sponge-like pores or additional pores. Increasing the ethanol content (in suspension) from 0 to 20 wt% leads to the shift of pore size (of finger-like pores) from 0.45 to 0.1 μm for fibres, indicating that finger-like voids either become smaller or are removed. Hollow fibres made from 20 wt% ethanol suspension and beyond show negligible pore formation. This might be closely associated with the viscosity as evidenced by the substantial viscosity increase upon adding 20 wt% ethanol into the suspension which tends to inhibit the viscous fingering phenomenon during phase inversion.

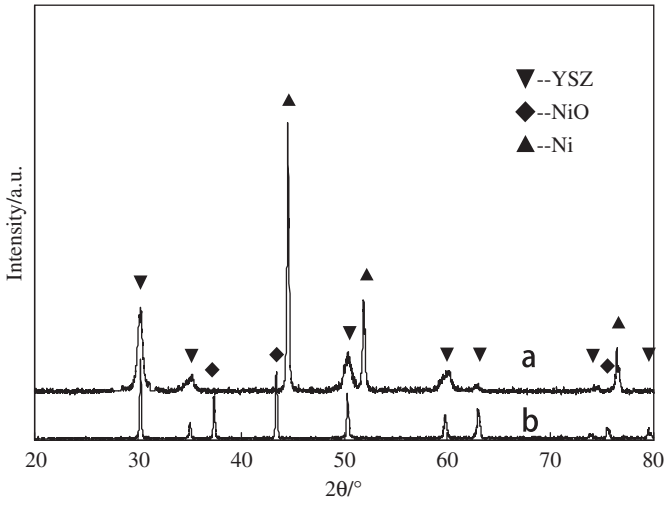

Fig. 7. Powder x-ray diffraction (XRD) of NiO/YSZ(b) and Ni/YSZ(a) hollow fibres.

Fig. 7 shows the typical powder XRD patterns of the sintered NiO/YSZ and Ni/YSZ hollow fibres. Here, only fibres made from suspensions containing 20 wt% ethanol are depicted due to the similarity (of the XRD patterns) to the other fibres. No extra reflections from other phases than the cubic YSZ and the cubic NiO in the NiO/YSZ hollow fibre sample (Fig. 7(a)) were noticed although the sintering temperature was quite high (1400 °C). The hollow fibre is therefore comprised of a mixture of NiO and YSZ with no other new phases formed during the spinning and sintering process. After reduction, characteristic peaks of NiO disappear and are replaced by characteristic peaks of Ni; denoting complete transformation of NiO particles into Ni metal.

Electrical conductivity is another important parameter towards using Ni/YSZ hollow fibres as anode support for SOFCs considering its role as the electrochemical reactions' site and current collector. The Ni/YSZ ceramic–metallic

contains two phases e.g. an electronic conductor, Ni and an ionic conductor, YSZ. To obtain high electrical conductivity and high-catalytic activity, both Ni and YSZ phases should form percolative (continuous) networks. If the percolative condition is satisfied, the overall conductivity would be contributed effectively by the Ni phase since the electronic conductivity of Ni is five orders of magnitude larger than the ionic conductivity of YSZ. Fig. 8 depicts the electrical conductivity of Ni/YSZ hollow fibres (acquired from average of three cermets measurements) as a function of temperature measured in reducing atmosphere. The electrical conductivity shows decreasing trend with increasing temperature; representing the dominant metallic behaviour of Ni. Taking into account low ionic conductivity of 8 YSZ ($\sim$0.15 Scm^{-1} at 1000 °C) [25], the observed high electrical conductivity and metallic behaviour is attributed to the formation of a continuous Ni phase within the fibres. Hollow fibres made from suspensions containing higher ethanol content demonstrate larger electrical conductivity than those made from suspensions containing less ethanol. For example, the fibre made from 35 wt% ethanol suspension sintered at 1400 °C shows a maximum electrical conductivity of 2840 Scm^{-1} at room temperature. This trend might be related to the electron conducting path of electron within the fibre, where the fibres with thicker sponge-layer structure are expected to have longer conduction paths. The lower porosity of Ni/YSZ also seems to provide superior electrical conductivity (not shown here) as suggested by the dependence of electrical conductivity of composites to porosity [26]:

$$\sigma_{tatal} = \sigma_b(1-p)^{3/2} \quad (3)$$

where σ_{tatal} is the total electrical conductivity, σ_b is the bulk electrical conductivity and p is porosity. The electrical conductivity of Ni/YSZ hollow fibre in this study is much larger than that found in the previous report [23]. Slightly different sintering temperatures and Ni content as well as the direct connection between hollow fibre and the testing setup utilised here might be responsible for the discrepancy. Still, the reported conductivity values here are less than those reported for Ni/CGO hollow fibres [21].

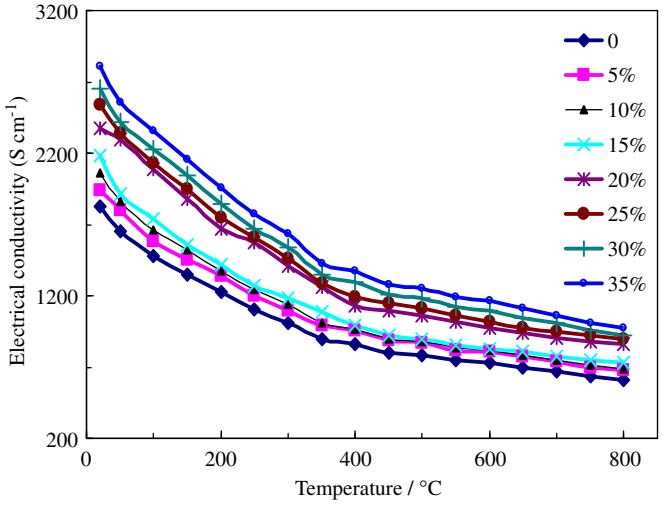

Fig. 8. Electrical conductivities of the reduced NiO/YSZ hollow fibre.

4. Conclusions

Microstructure evolution of the Ni–YSZ hollow fibres prepared using phase inversion sintering-technique is studied as a function of ethanol addition into spinning suspensions. By adjusting the ethanol content (as a non-solvent), the microstructure of the resultant hollow fibres can be manipulated due to the differences in coagulation effect and viscosity of suspensions. Adding ethanol brings significant changes in the viscosity when the ethanol is added beyond 5 wt% (of suspensions). The hollow fibre exhibits structure evolution from two thin outer sponge-like layers sandwiching a finger-like inner layer to a dominant single sponge-like layer upon increasing the ethanol amount from 0 to 35 wt%. This morphology change also correlates with the change in hollow fibre properties and performance, in particular, porosity, shrinkage, mechanical strength and electrical conductivity change from 67% to 28%, 44% to 20%, 94 to 250 MPa and 1890 to 2540 Scm^{-1}, respectively (all at room temperature) by increasing ethanol from 0 wt% to 35 wt%. Hollow fibres made utilising 15–20 wt% of ethanol (in suspensions) are considered the most attractive option for MT-SOFCs from the optimum porosity perspective.

Acknowledgements

The authors gratefully acknowledge research funding from Natural Science Foundation of China (no. 20976098, 21076118, 21173147), Tianjin Natural Science Foundation (11JCZDJC23400) and Promotive Research Fund for Excellent Young and Middle-aged Scientists of Shandong Province (no. 2010BSB01011).

References

[1] Z. Shao, S.M. Haile, J. Ahn, P.D. Ronney, Z. Zhan, S.A. Barnett, A thermally self-sustained micro solid-oxide fuel-cell stack with high power density, Nature 435 (2005) 795–798.
[2] A. Atkinson, S. Barnett, R.J. Gorte, J.T.S. Irvine, A.J. Mcevoy, M. Mogensen, S.C. Singhal, J. Vohs, Advanced anodes for high-temperature fuel cells, Nature Materials 3 (2004) 17–27.
[3] K.F. Chen, Y.T. Tian, Z. Lü, N. Ai, X.Q. Huang, W.H. Su, Behavior of 3 mol% yttria-stabilized tetragonal zirconia polycrystal film prepared by slurry spin coating, Journal of Power Sources 186 (2009) 128–132.
[4] I.R. Gibson, G.P. Dransfield, J.T.S. Irvine, Influence of yttria concentration upon electrical properties and susceptibility to ageing of yttria stabilized zirconias, Journal of the European Ceramic Society 18 (1998) 661–667.
[5] K. Kendall, M. Palin, A small solid oxide fuel cell demonstrator for microelectronic applications, Journal of Power Sources 71 (1998) 268–270.
[6] M.A. Laguna-Bercero, R. Campana, A. Larrea, J.A. Kilner, V.M. Orera, Electrolyte degradation in anode supported microtubular

yttria stabilized zirconia-based solid oxide steam electrolysis cells at high voltages of operation, Journal of Power Sources 196 (2011) 8942–8947.
[7] V. Lawlor, S. Griesser, G. Buchinger, A.G. Olabi, S. Cordiner, D. Meissner, Review of the micro-tubular solid oxide fuel cell Part I. Stack design issues and research activities, Journal of Power Sources 193 (2009) 387–399.
[8] K. Kendall, Progress in microtubular solid oxide fuel cells, International Journal of Applied Ceramic Technology 7 (1) (2010) 1–9.
[9] L. Liu, X. Tan, S. Liu, Yttria stabilized zirconia hollow fibre membranes, Journal of the American Ceramic Society 89 (3) (2006) 1156–1159.
[10] Y. Liu, O.Y. Chen, C.C. Wei, K. Li, Preparation of yttria-stabilized zirconia (YSZ) hollow fibre membranes, Desalination 199 (2006) 360–362.
[11] C.C. Wei, K. Li, Yttria-stabilized zirconia (YSZ)-based hollow fiber solid oxide fuel cells, Industrial and Engineering Chemistry Research 47 (2008) 1506–1512.
[12] K. Kanawka, F.D. Grande, Z.T. Wu, A. Thursfield, D. Ivey, I. Metcalfe, G. Kelsall, K. Li, Microstructure and performance investigation of a solid oxide fuel cells based on highly asymmetric YSZ microtubular electrolytes, Industrial and Engineering Chemistry Research 49 (2010) 6062–6068.
[13] X. Tan, Y. Liu, K. Li, Preparation of LSCF ceramic hollow fiber membranes for oxygen production by a phase-inversion/sintering technique, Industrial and Engineering Chemistry Research 44 (2005) 61–66.
[14] K. Li, X. Tan, Y. Liu, Single-step fabrication of ceramic hollow fibers for oxygen permeation, Journal of Membrane Science 272 (2006) 1–5.
[15] C. Jin, C. Yang, F. Chen, Effects on microstructure of NiO-YSZ anode support fabricated by phase-inversion method, Journal of Membrane Science 363 (2010) 250–255.
[16] N.T. Yang, X. Tan, X.X. Meng, Y. Yin, Z.F. Ma, Fabrication of anode supported micro tubular SOFCs by dip-coating process on NiO/YSZ hollow fibers, ECS Transactions 25 (2) (2009) 811–888.
[17] C. Yang, W. Li, S. Zhang, L. Bi, R. Peng, C. Chen, W. Liu, Fabrication and characterization of an anode-supported hollow fiber SOFC, Journal of Power Sources 187 (1) (2009) 90–92.
[18] C. Chen, M. Liu, L. Yang, M. Liu, Anode-supported micro-tubular SOFCs fabricated by a phase-inversion and dip-coating process, International Journal of Hydrogen Energy 36 (9) (2011) 5604–5610.
[19] U. Doraswami, P. Shearing, N. Droushiotis, K. Li, N.P. Brandon, G.H. Kelsall, Modelling the effects of measured anode triple-phase boundary densities on the performance of micro-tubular hollow fiber SOFCs, Solid State Ionics 192 (2011) 494–495.
[20] B.F.K. Kingsbury, K. Li, A morphological study of ceramic hollow fibre membranes, Journal of Membrane Science 328 (1–2) (2009) 134–140.
[21] M.H.D. Othman, Z. Wu, N. Droushiotis, G. Kelsall, K. Li, Morphological studies of macrostructure of Ni–CGO anode hollow fibres for intermediate temperature solid oxide fuel cells, Journal of Membrane Science 360 (2010) 410–417.
[22] T. Schiestel, M. Kilgus, S. Peter, K.J. Caspary, H. Wang, J. Caro, Hollow fibre perovskite membranes for oxygen separation, Journal of Membrane Science 258 (2005) 1–4.
[23] N. Yang, X. Tan, Z. Ma, A phase inversion/sintering process to fabricate nickel/yttria-stabilized zirconia hollow fibers as the anode support for micro-tubular solid oxide fuel cells, Journal of Power Sources 183 (2008) 14–19.
[24] D. Dong, J. Gao, X. Liu, G. Meng, Fabrication of tubular NiO/YSZ anode-support of solid oxide fuel cell by gel casting, Journal of Power Sources 165 (2007) 217–223.
[25] M. Han, X. Tang, H. Yin, S. Peng, Fabrication, microstructure and properties of a YSZ electrolyte for SOFCs, Journal of Power Sources 165 (2007) 757–763.
[26] D.A.G. Bruggeman, Berechnung verschiedener physikalischer Konstanten von heterogenen Substanzen, Annals of Physics (Amsterdam, Netherlands) 24 (1935) 636–679.